



## Research Article

# Simultaneous electricity generation and removal of Sars-Cov-2 from wastewater in microbial fuel cells

Sıla ARSLAN<sup>1</sup>, Tunç ÇATAL\*<sup>1</sup>

<sup>1</sup>Department of Molecular Biology and Genetics, Uskudar University, İstanbul, 34662, Türkiye

## ARTICLE INFO

### Article history

Received: 02 August 2024

Revised: 03 October 2024

Accepted: 18 November 2024

### Keywords:

SARS-CoV-2; Wastewater;  
Microbial Fuel Cells; S1 Protein;  
Bioremediation

## ABSTRACT

In this study, whether wastewater contaminated with SARS-CoV2 virus can be disinfected using microbial fuel cells was modeled using the S1 anchor protein of the virus. The disinfection potential and simultaneous electricity production of wastewater contaminated with SARS-CoV-2 mixed with wastewater using microbial fuel cells, an innovative technology, were investigated. Bioremediation of SARS-CoV-2 contaminated wastewater was modeled using SARS-CoV-2 surface antigen (S1) and studied in microbial fuel cells at different temperatures (30 °C vs. 25 °C). Our results show that microbial fuel cells gradually reduced the SARS-CoV-2 viral concentration from 213 ng/mL, especially at ambient temperature, and simultaneously achieved a power density of  $184.19 \pm 21.31$  mW/m<sup>2</sup> at a current density of  $0.073 \pm 0.029$  mA/cm<sup>2</sup>. The log reduction rates of closed-circuit microbial fuel cells increased steadily from 0.005 to 0.163. In conclusion, microbial fuel cells can be used to simultaneously generate electricity to enable biological treatment of wastewater contaminated by SARS-CoV-2.

**Cite this article as:** Arslan S, Çatal T. Simultaneous electricity generation and removal of Sars-Cov-2 from wastewater in microbial fuel cells. Sigma J Eng Nat Sci 2026;44(1):252–261.

## INTRODUCTION

Due to the world's ever-increasing population and industrialization trend, global water availability and energy consumption have become important topics of discussion. The world population is growing rapidly and is expected to increase by another 21% by 2040. As a result, both the need for clean water and the need for energy are increasing. Fossil fuels are widely used to meet energy needs but are becoming increasingly depleted, so alternative energy sources are needed [1]. Similarly, water scarcity remains a major problem worldwide, and the Earth's freshwater resources may

decrease by 40% in the next decade [2]. Since organic waste is a viable energy source, wastewater has become a renewable energy source with minimal environmental impact. Microbial fuel cell (MFC) technology, which has versatile features, is a technology on which intensive research has been carried out in recent years, as it enables the production of electricity from organic waste and contributes to the simultaneous production of clean water [3-5]. In microbial fuel cells, microorganisms called exoelectrogens release electrons and protons while breaking down carbon sources in organic waste materials as substrates [6-7-8]. These released electrons are taken by an anode and transferred to

### \*Corresponding author.

\*E-mail address: [tunc.catal@uskudar.edu.tr](mailto:tunc.catal@uskudar.edu.tr)

This paper was recommended for publication in revised form by Editor-in-Chief Ahmet Selim Dalkilic



the cathode through the external circuit. Protons also reach the cathode through the medium solution and react with electrons in the presence of oxygen to form water. Electrical energy is generated as electrons flow through the external circuit. In addition, the breakdown of organic waste and the formation of water by cathodic reaction allows wastewater treatment. Thanks to these versatile features, microbial fuel cells have the potential to support operating costs by being integrated into wastewater treatment plants. By using microbial fuel cells, which are a clean technology, antibiotics, heavy metals, drug metabolites, or various environmental pollutants mixed into wastewater, the ecosystem can be cleaned [9–11]. As a recent contaminant, the detection and disinfection of SARS-CoV-2 viruses, a significant risk, in wastewater has drawn attention to this issue.

After infection by the SARS-CoV-2 virus [12], which has affected all humanity and emerged with life-threatening effects in recent years, viral proteins in gastrointestinal epithelial biopsy samples and virus detection in stool samples have been reported [13]. The effects of COVID-19 on various patients are still being investigated [14], and using actual data, deterministic COVID-19 models were examined to assess the effects of COVID-19 and dynamic transmission [15]. Viral RNA can be found in the feces of approximately 40% of infected individuals [16]. SARS-CoV-2 can be detected in stool samples for longer periods than the virus can be detected in nasal swab samples [16]. Some studies have reported that SARS-CoV-2 survives longer in the urine of infected individuals than in their feces [17]. Accordingly, the SARS-CoV-2 virus in wastewater was investigated [18]. The first detection of SARS-CoV-2 in wastewater was achieved by qRT-PCR testing, isolating it from municipal wastewater in six different cities in the Netherlands. Viral load in wastewater varies by region. In settlements close to sampling sites, the number of viral genomes detected in wastewater has been reported to increase at the regional level due to COVID-19-related hospitalizations [19]. A study by Škulcová et al. [20] reported that the SARS-CoV-2 virus was detected in hospital wastewater, and the relevant virus was detected in the feces of 40% to 89% of COVID-19 patients. Samples taken over six-day periods from a wastewater plant in Australia resulted in two positive results for the presence of SARS-CoV-2 [21]. Additionally, Guerrero-Esteban et al. [22] state that the detection of S1 protein in rivers and wastewater is possible. The immunosensor detects spike protein at the pg/ml level. Miyani et al. [23] investigated the amount of SARS-CoV-2 with concentrations of  $10^4$ – $10^5$  genomic copies/L in wastewater. An average of  $3.10^6$  genome units per liter were detected in SARS-CoV-2 samples from various wastewater treatment plants [24]. Wurtzer et al. [24] reported that the concentration of SARS-CoV-2 increased from  $5 \times 10^4$  copies/L to  $3 \times 10^6$  genome units per liter in a wastewater treatment plant.

In another wastewater treatment plant, SARS-CoV-2 viral RNA N1 and N2 gene regions are quantified in

wastewater solids in water resource recovery facilities [25]. The presence of SARS-CoV-2 in sewers has been identified as an indicator of the potential for the virus to transmit to humans [26]. The Omicron variant was detected in aircraft wastewater [27]. According to a study conducted in 2022, the Omicron variant was found in a wastewater treatment plant [28]. Another study reported an adaptable protocol to monitor SARS-CoV-2 variants in wastewater with high sensitivity and specificity [29]. Various techniques have been proposed to eliminate SARS-CoV-2 from wastewater because it poses a risk to the environment and human health. For example, techniques such as chlorine dioxide, liquid chlorine, sodium hypochlorite, ozone, ultraviolet, and ultrafiltration have been proposed to purify wastewater from SARS-CoV-2 viral load [19]. However, retardation, dispersion, inactivation, and degradation can all have an impact on the destiny of viruses in wastewater. Temperature is the primary factor influencing virus survival [30]. A shorter viral lifespan in the sewage is caused by an increase in the inactivation rate coefficient with temperature [30]. As a disinfection method, microbial fuel cell technology has been proposed to disinfect human urine contaminated with viral load [31]. However, this study is the first in the literature, as there has been no research on SARS-CoV-2 disinfection and simultaneous electricity production using microbial fuel cells. In this regard, this study is novel in that it suggests, for the first time, that SARS-CoV-2-contaminated wastewater can be disinfected and electricity generated using MFCs.

This study used the S1 protein, the protein's surface antigen of the SARS-CoV-2 virus, to model wastewater contaminated with SARS-CoV-2. The electrical performances of MFCs were evaluated at different temperatures simultaneously with the biological treatment of modeled polluted wastewater. ELISA testing was used to measure the concentration of SARS-CoV-2 viral proteins during operation in MFCs.

## MATERIALS AND METHODS

### Materials

#### Inoculation of microbial fuel cells (MFCs)

The single-chamber MFC was prepared per the research procedure published in a previous report [3]. Plexiglass, a plastic glass material, was utilized to construct the MFC. The plexi cube had a total volume of 12 mL. The anode's plexi cover was entirely closed and designed so it would not come into contact with oxygen. This procedure was carried out to prevent oxygen from leaking into the anode region. Carbon cloth was cut to  $7 \text{ cm}^2$  for it to operate as an anode and a cathode. The anode was made of carbon fabric (Cat. no: 14032102, FuelCells, Texas, USA). The cathode material consisted of coarse carbon cloth (Cat. no: CTO32414, FuelCells, Texas, USA) covered with Nafion

(5%, Sigma–Aldrich, 7 mL per mg of Pt/C catalyst) and platinum (Pt) (20 wt% Pt/C Vulcan XC-72, FuelCell Store, USA) [32,33]. A synthetic wastewater consisting of sodium phosphate buffer (100 mM strength at pH 7.4) and sodium acetate trihydrate (20 mM) ( $C_2H_3NaO_2 \cdot 3H_2O$ , VWR Chemicals, Product No: 27652.298, Batch: 15D140018, Geldenaaksebaan, Leuven, Belgium) was prepared [34]. Activated sludge was obtained from a local domestic wastewater treatment plant (Pasakoy, Advanced Biological Wastewater Treatment Plant, Istanbul, Türkiye) [35]. The computer-aided data acquisition system (Keithley KickStart Software, Version 1.9.8.21, Tektronix Company, Beaverton, Oregon, USA) recorded voltage data. The KickStart program was designed to collect data every 11 minutes. MFCs ( $n=2$ ) operated at 37 °C and 25 °C.

#### Modeling of contaminated wastewater with SARS-CoV-2

SARS-CoV-2 S1 protein (Nepenthe Research Technologies, Ref No: E91011) was used to model the SARS-CoV-2 contaminated wastewater in synthetic wastewater. 23  $\mu$ L of S1 protein at 1.13 g/mL concentration was kept at -20 °C until use. To detect the wastewater contaminated with SARS-CoV-2, an enzyme-linked immunosorbent assay (ELISA) kit (Nepenthe Research Technologies, 96 tests, Ref No: NE0000211101) research was carried out.

The concentration of S1 protein to be used for SARS-CoV-2 contaminated wastewater modeling was 213 ng/mL [36].

#### Operation of MFCs

MFCs were operated at 30 °C and 25 °C temperatures using an external resistance of 985  $\Omega$  in a batch mode. Three and a half hours of operation were completed by sampling 100  $\mu$ L samples from the reactors at half-hour intervals [31]. All MFCs were examined to monitor the disinfection. The entire operational time was judged to be 40 minutes. Every 10 minutes, 100  $\mu$ L of the sample was collected. Current ( $I=V/R$ ) and power ( $P=I \cdot V$ ) densities were calculated using voltage (V) data according to Ohm's law and normalized to the electrode surface area at different external resistances (R) [37].

#### ELISA Application

After the microbial operations were performed, eight different concentrations of S1 standard were prepared by serial dilution technique using the S1 antigen standard solution and blocking solution included in the ELISA kit to determine the concentrations of the samples by creating a standard graph other than the collected samples. ELISA was performed following the kit protocol (Nepenthe Co., Istanbul). Absorbance was measured at 450 nm with a microplate reader (Thermo Scientific, Multiskan Go, Microplate Spectrophotometer). The GraphPad Prism 7.0.0 program was used to calculate the concentration of absorbance data for each sample. The concentration of each sample was determined using the obtained absorbance values. The log reduction was calculated using the pre-operative

and post-operative concentrations. The log reduction formula was used as outlined in the study by Pasternak et al. [31]:

$$LR = \text{Log}_{10}(A/B)$$

A equals the antigen concentration of the sample before the operation, and B equals the antigen concentration of the sample after the procedure.

#### Calculation of Statistical Data

The t-test p-values were computed using n-Whitney test on the MFCs run using the GraphPad Prism 7.0.0 software. A p-value less than 0.05 indicates that the result is/were determined. In contrast, the t-test reveals whether the findings are substantially different. The time-dependent SARS-CoV-2 concentration and the t-test p-value of the SARS-CoV-2 virus's log reduction rate was determined as a result.

## RESULTS AND DISCUSSION

#### MFC Performances and Effects of SARS-CoV-2 Proteins on Electricity Generation

Only 20 mM sodium acetate as the sole carbon source was inoculated into MFC until stable, and consistent voltage data was obtained (for 134 days). During this period, up to 0.394 V of electricity was produced at 30 °C (Fig. 1A). At ambient temperature (25 °C), the outcome of the produced voltage was tracked. The maximum voltage at 25 °C was 0.3810 V (Fig. 1B) at 985 Ohm external resistance. To assess the current and power density, external resistances with varied Ohm values (1204  $\Omega$ , 985  $\Omega$ , 646  $\Omega$ , 325  $\Omega$ , and 215  $\Omega$ ) were examined. The maximum power density was 145 mW/m<sup>2</sup> at the current density level of 0.05 mA/cm<sup>2</sup> at 30 °C, where the power density increased when the temperature decreased to 25 °C (210 mW/m<sup>2</sup>) (Fig. 2B).

These results indicate that temperature has an effect on voltage generation and power generation in microbial fuel cells. Synthetic wastewater contaminated with SARS-CoV-2 protein was fed to the MFC at 30 °C, and the voltage data was monitored. Under the 30 °C temperature condition, no significant change in voltage production was observed when SARS-CoV-2 protein was introduced into MFCs. Voltage production levels remained at 0.36 V under 30 °C temperature conditions. The maximum voltage produced was 0.36 V. SARS-CoV-2 polluted wastewater modeling at ambient temperature and ambient temperature was performed in the MFC with a 20 mM acetate inoculation solution. However, an instantaneous increase in voltage production was detected when the SARS-CoV-2 viral protein was added to synthetic wastewater at 25 °C (Fig. 3). These findings suggested whether microbial fuel cells could be used as biosensors for the presence of SARS-CoV-2 in wastewaters.

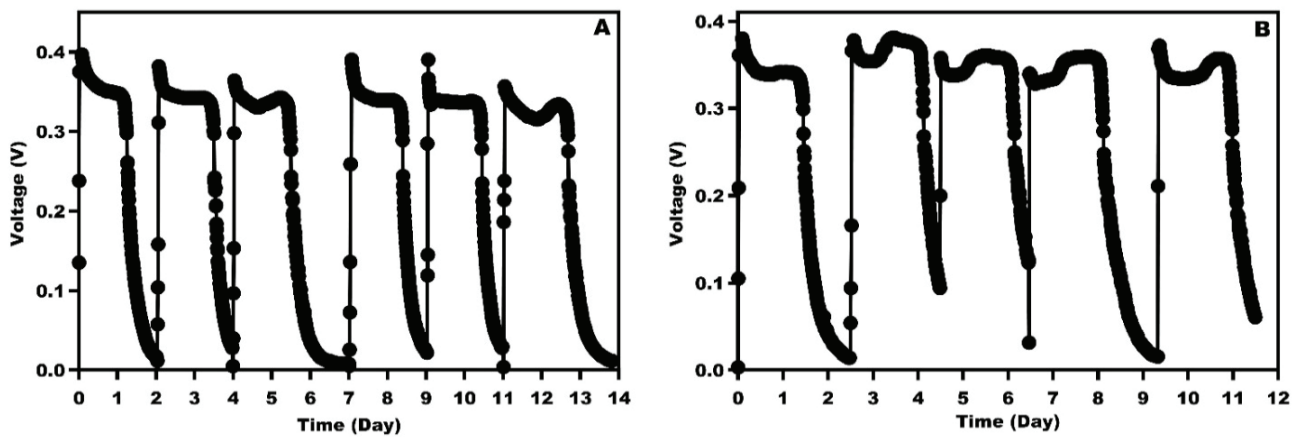


Figure 1. Voltage versus time data of MFC with 985 Ω external resistance at controlled temperature (A), Voltage versus time data of MFC with 985 Ω external resistance at ambient temperature.

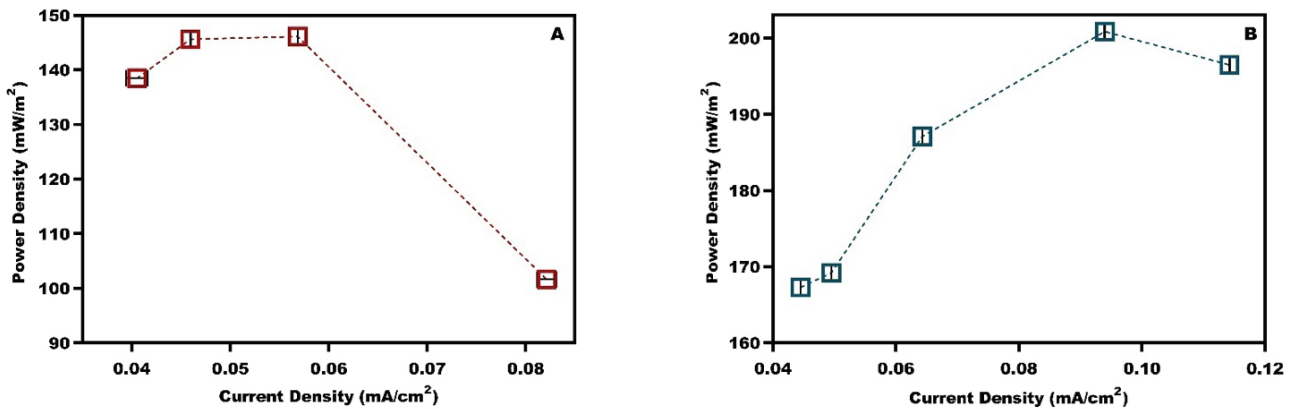


Figure 2. MFC performances at 30 °C (A), and at 25 °C (B).

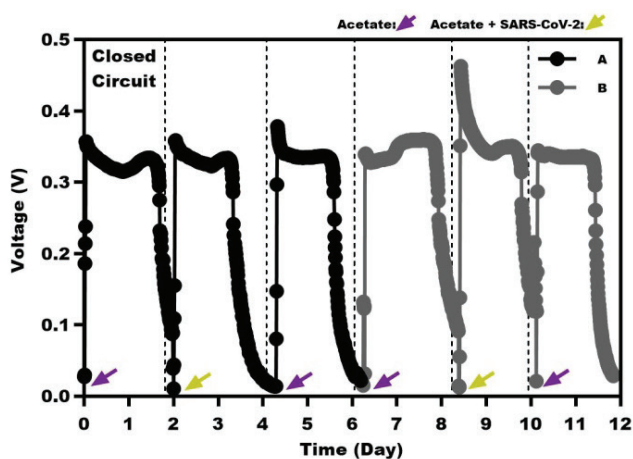


Figure 3. Voltage during the operation plot of SARS-CoV-2 contaminated wastewater modeling at 30 °C temperature (A) and 25 °C (B). Yellow arrow indicates the addition of SARS-CoV-2 S1 protein.

### Removal of SARS-CoV-2 Viral Protein in MFCs

Following ELISA, a standard curve was produced based on the absorbance of S1 antigen concentrations at 450 nm ( $OD_{450}$ ). A total of eight S1 antigen concentrations were used. The created standard curve had an  $R^2$  value of 0.9967. Figure 4 shows the standard curve plot of the S1 antigen.

At 30 minutes, the concentration of SARS-CoV-2 in the MFC decreased to 47 ng/mL. Under the 30 C temperature condition, S1 protein concentration rapidly decreased (47 ng/L). Concentration levels remained at this level for the 210th minute. However, when the operating temperature was reduced to 25 °C, the decrease in S1 concentration slowed down. At a temperature of 25 °C, S1 concentration reached 180 ng/L. These findings showed that operating temperature is an important parameter in the disinfection of wastewater contaminated with SARS-CoV-2. MFC log reduction rates were computed on an hourly basis. The substantial log reduction rate implied that the SARS-CoV-2 virus was successfully removed. The log reduction rate of

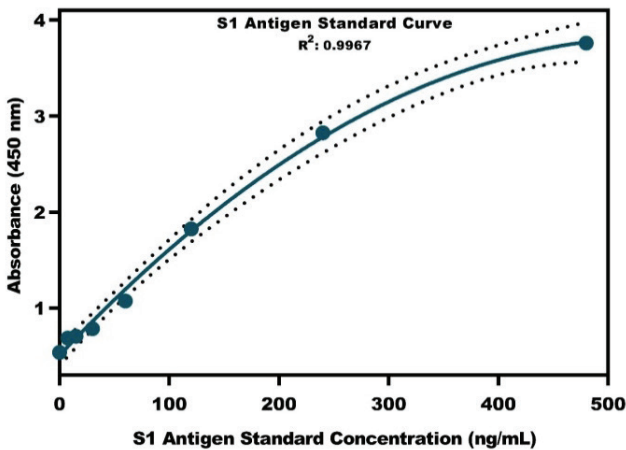


Figure 4. The standard curve plot of S1 antigen.

the MFC after half an hour at 30 °C temperature was 1.40. After three and a half hours, it was measured as 0.17. The rate of log reduction steadily reduced (Fig. 5). These results suggest that SARS-CoV-2 viral proteins are removed in MFCs.

At 30 minutes, the concentration of SARS-CoV-2 in the closed circuit MFC decreased to 47 ng/mL, while the virus concentration in the abiotic control MFC decreased to 21 ng/mL. At the end of one hour, the SARS-CoV-2 concentration in the closed circuit had risen to 49 ng/mL, whereas the abiotic control had a concentration of 23 ng/mL. After an hour and a half, the SARS-CoV-2 concentration in the closed-circuit MFC sample was 64 nanograms per milliliter. The abiotic control sample obtained simultaneously had a concentration of 36 ng/mL. The fifth sample was obtained from both MFCs after two hours. The concentration of MFC' in these samples was reduced to 58 ng/mL for the closed circuit MFC' and 15 ng/mL for the abiotic control MFC. The fifth sample was obtained from both MFCs after

two hours. The concentration of MFC' in these samples was reduced to 58 ng/mL for the closed circuit MFC' and 15 ng/mL for the abiotic control MFC. The concentration of SARS-CoV-2 contaminated wastewater in the closed circuit MFC was 61 ng/mL after two and a half hours. The concentration of SARS-CoV-2 in the abiotic circuit was 12 ng/mL. Three hours later, the viral concentration in the closed circuit MFC was 65 ng/mL. The appropriate concentration for the abiotic control MFC was 25 ng/mL. The operation of the simulated slater concluded three and a half hours later, with the collection of the final sample. The ultimate sample concentration of MFC in the closed circuit was 59 ng/mL. SARS-CoV-2 was found at a concentration of 43 ng/mL in the final sample of abiotic control MFC (Fig. 6).

A novel approach was established for MFCs at ambient temperature based on the operation ELISA findings of MFCs at controlled temperature. The entire operating time in this newly created approach was lowered to forty

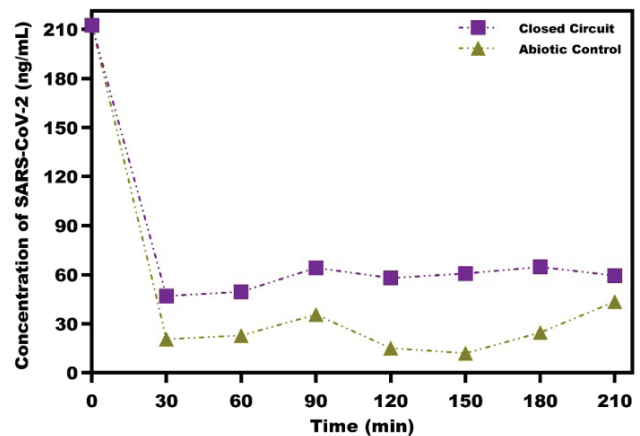


Figure 6. Time-dependent concentration graph of MFC at controlled temperature throughout the operation.

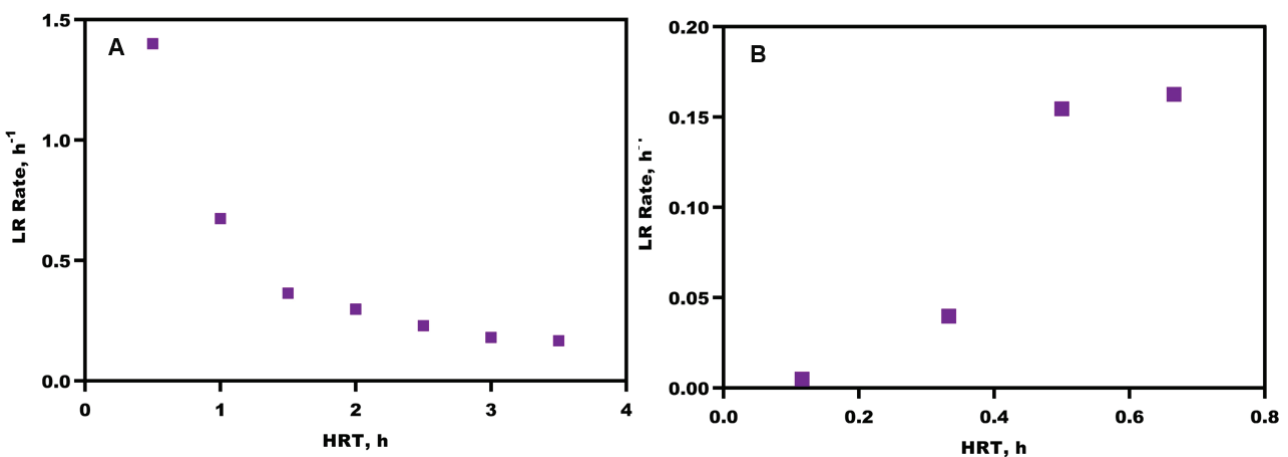
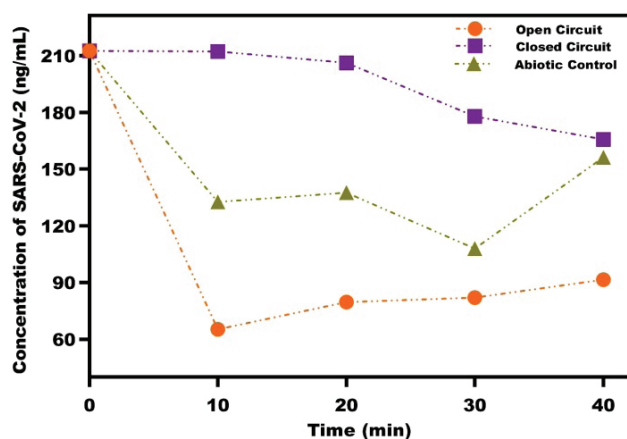


Figure 5. Graph of log reduction of MFCs at 30 °C temperature (A). Graph of log reduction of MFCs at 25 °C.

minutes, and sample periods were updated to every ten minutes. Given the findings at controlled temperature, it was decided to install an additional circuit (open circuit MFC). The SARS-CoV-2 concentration at which each MFC began functioning was 213 ng/mL. Within the first 10 minutes, the concentration of open-circuit MFC dropped to 65 ng/mL, the closed-circuit open-circuit MFC dropped to 65 ng/mL, the closed-circuit MFC to 213 ng/mL, and the abiotic control MFC to 133 ng/mL. The SARS-CoV-2 concentration of open circuit and abiotic control MFCs rose 20 minutes after the surgery, but the concentration of closed MFCs continued to drop. At 20 minutes, the open circuit MFC concentration was 80 ng/mL. The SARS-CoV-2 concentration in the closed circuit MFC was 206 nanograms per milliliter, whereas it was 138 ng/mL in the abiotic control. Thirty minutes later, the open circuit MFC concentration was determined to be 82 ng/mL. The concentrate circuit closed-circuit MFC steadily decreased, and the SARS-CoV-2 concentration was 178 ng/mL at the end of half an hour. After thirty minutes, the abiotic control MFC had a deadly viral concentration of 108 ng/mL. The concentration of open circuit and abiotic control MFCs continued to grow during the forty-first minute of the operation, whereas it continued to drop in the closed circuit MFCs. In the fortieth minute of the open circuit MFC,



**Figure 7.** Time-dependent concentration graph of MFC at ambient temperature throughout the operation.

the SARS-CoV-2 concentration climbed to 92 ng/mL. In a closed circuit MFC, the SARS-CoV-2 concentration was determined to be 116 ng/mL. In the last ten minutes, the concentration of SARS-CoV-2 in the abiotic control MFC reached 156 ng/mL. This rate represents an exceptional rise in past operations' outcomes. At the end of the forty-first minute, the abiotic control MFC's SARS-CoV-2 concentration was nearly equivalent to the closed circuit MFC, which declined gradually and methodically (Fig. 7).

The detection of SARS-CoV-2 in wastewater has been reported previously, and the presence of SARS-CoV-2 in wastewater increases the potential spread. However, the need for SARS-COV-2 removal from wastewater has arisen. Within the scope of the large-scale study by Acosta et al. (2021), wastewater samples were collected twice a week from three different hospitals for four months [38]. It has been reported that the amount of SARS-CoV-2 in wastewater is directly proportional to hospitalizations due to COVID-19 cases [38]. The presence and amount of SARS-CoV-2 in the wastewater where the treated water from the wastewater treatment plant mixes into the river, depending on the number of hospitalizations of COVID-19-related cases in the hospital [39], and the SARS-CoV-2 virus was also found in river water and with a high detection frequency. Thus, it has been reported that treating treated wastewater mixed with river water may not be sufficient [39]. The effects of currently used wastewater treatment methods on SAR, such as chlorination of wastewater, ultraviolet (U.V.) irradiation, membrane technology, and advanced oxidation processes the effect of temperature on voltage production in MFCs, were the effect of temperature on voltage production in MFCs was the effect of temperature on voltage production in MFCs was reported and showed that it has an impact on power production [40]. Pasternak et al. [31], a deadly pathogen and biological contaminant, succeeded in separating the hepatitis B virus from human urine and generating electricity using MFCs [31]. Enough removal of hepatitis B viruses by microbial fuel cells was reported to reduce the risk of viral spread. However, they stated that they needed to apply the method they developed to different kinds of viruses to make the results more explainable. The log reduction rate calculated by Pasternak et al. [31] for the surface antigen started from almost 5 for the closed

**Table 1.** Comparison of MFC performances for disinfection of various contaminants

Disinfected material	MFC Type	Power density	Current density	Removal efficiency	References
SARS-CoV2	Single chamber air-cathode MFCs	184.19±21.31	0.073±0.029	78%	This study
Hepatitis virus	Single chamber air-cathode MFCs	n.a.	n.a.	99.99%	[31]
Ammonia/nitrate/nitrite	Sediment MFC	1794	1.1	~100%/ 65%/~90%	[41]

n.a.: not available

**Table 2.** The statistical significance of the difference between time-dependent concentration values of S1 antigen of MFCs (\*). The statistical significance of the difference between SARS-CoV-2 log reduction values of MFCs (\*\*)

	Controlled Temp.		Ambient Temp.	
	Closed Circuit vs. Abiotic Control	Open Circuit vs. Closed Circuit	Closed Circuit vs. Abiotic Control	Open Circuit vs. Abiotic Control
t-test p-value*	0.007	0.01	0.05	0.22
t-test p-value**	0.0012	0.03	0.03	0.03

circuit MFC. The log reduction rates of hepatitis B virus surface antigen gradually decreased for both MFCs [31]. In our study, the first log reduction rate of the closed circuit MFC in a temperature environment of  $30\pm 2^\circ\text{C}$  was 1.40. While the initial SARS-CoV-2 log reduction rate calculated for the closed circuit MFC at room temperature was 0.005, this rate increased gradually throughout the operation period. It reached 0.163 at the end of forty minutes. The difference in log reduction between the study of Pasternak et al. [31] and our study at room temperature is thought to be due to the different biofilm structures of MFCs or the difference in the viruses used [31–41].

These results suggest that external factors such as temperature and MFC configuration may affect the disinfection of SARS-CoV-2, where simultaneous electricity can be generated.

The t-test p-value of the closed circuit MFC and abiotic control reactor in a controlled temperature environment was 0.007, and the time-dependent SARS-CoV-2 concentration data of the two bioreactors differed considerably. Three distinct MFC time-dependent SARS-CoV-2 concentration values at ambient temperature were statistically compared. The t-test p-value for closed-circuit MFC and open-circuit MFC was 0.01, suggesting that they varied substantially. Again, at ambient temperature, the t-test p-value of the closed circuit MFC and abiotic control bioreactors was 0.05, and the time-dependent concentration values were not substantially different. Finally, the t-test p-value of 0.22 showed that the time-dependent SARS-CoV-2 concentration data from open MFC and abiotic control bioreactor were not significantly different (Table 1).

The t-test p-value for SARS-CoV-2 log reduction values of the closed circuit MFC and abiotic control bioreactors in a controlled temperature environment was 0.0012, showing a significant difference between the two bioreactors. In an ambient temperature setting, the t-test p-value findings of the SARS-CoV-2 log reduction values of three distinct MFCs were comp circuit circuit open-circuit MFC and closed-circuit MFC was 0.03, and the log reduction difference was significant. Closed circuit MFC and abiotic control had a t-test p-value of 0.03, indicating a significant difference between these two bioreactors. Lastly, at ambient temperature, the t-test p-value of the open circuit MFC

and abiotic control was determined to be 0.03. This finding indicates that the log reduction value of the SARS-CoV-2 virus differs significantly across the two MFCs (Table 1). Not only viruses but also other contaminants can be treated in MFCs. The efficiency and efficacy of heavy metal removal from wastewater are anticipated to be substantially improved by current research endeavors and advancements in MFC technology [42]. It is highly conceivable that autonomous wastewater treatment plants and MFCs—capable of remotely detecting—will be used in the future [43]. For this purpose, MFC technology can support the development of biosensors that can perform target-oriented detection. Our findings on eliminating SARS-CoV-2 from wastewater represent a substantial improvement in public health protection and environmental sustainability. By incorporating MFCs into wastewater treatment facilities, we can improve disinfection while decreasing virus loads and creating renewable energy. These findings have far-reaching ramifications, advising policymakers about new policies prioritizing pathogen elimination in wastewater management. Furthermore, MFC technology may be used to remove different types of organisms.

## CONCLUSION

In conclusion, the concentration of SARS-CoV-2 protein declined progressively over the operation duration of the microbial fuel cells, which were operated in a  $25^\circ\text{C}$  temperature environment. It did not rise during the operating period of the other examined reactors. Simultaneously, the log decrease rate progressively and steadily increased. In addition to all of this, the power generation efficiency was fairly great. As a result, it was determined that microbial fuel cells, running at a temperature of  $25^\circ\text{C}$  ambient temperature, executed the treatment of SARS-CoV-2 contaminated wastewater in a steady and circulatory manner, the bio removal of SARS-CoV-2 was accomplished, and there was considerable power production. Various parameters are needed for our promising work to be developed and extensively used. It is hoped that researching how diseases are removed at the molecular level may pave the way for more effective removal and eradication of additional pathogens. This study gives information on the real investigation of

SARS-CoV-2 polluted wastewater in advance. Furthermore, bioremediation of SARS-CoV-2 polluted wastewater using microbial fuel cells is expected to limit the production of new variants. Our findings suggest that novel microbial biosensors could be developed to detect the SARS-CoV-2 virus in wastewater.

## AUTHORSHIP CONTRIBUTIONS

Authors equally contributed to this work.

## DATA AVAILABILITY STATEMENT

The authors confirm that the data that supports the findings of this study are available within the article. Raw data that support the finding of this study are available from the corresponding author, upon reasonable request.

## CONFLICT OF INTEREST

The author declared no potential conflicts of interest with respect to the research, authorship, and/or publication of this article.

## ETHICS

There are no ethical issues with the publication of this manuscript.

## STATEMENT ON THE USE OF ARTIFICIAL INTELLIGENCE

Artificial intelligence was not used in the preparation of the article.

## REFERENCES

- [1] Naseer MN, Zaidi AA, Khan H, Kumar S, Owais MT, Jaafar J, et al. Mapping the field of microbial fuel cell: A quantitative literature review (1970-2020). *Energy Rep* 2021;4:126–4138. [\[CrossRef\]](#)
- [2] Gupta S, Srivastava P, Patil SA, Yadav AK. A comprehensive review on emerging constructed wetland coupled microbial fuel cell technology: Potential applications and challenges. *Bioresource Technol* 2021;124:376. [\[CrossRef\]](#)
- [3] Catal T, Liu H, Kilinc B, Yilancioglu K. Extracellular polymeric substances in electroactive biofilms play a crucial role in improving the efficiency of microbial fuel and electrolysis cells. *Appl Microbiol* 2024;77. [\[CrossRef\]](#)
- [4] Durna Piskin E, Genc N. Microbial fuel cells in electricity generation with waste treatment: Alternative electron acceptors. *Sigma J Eng Nat Sci* 2024;42:273–288. [\[CrossRef\]](#)
- [5] Sukkasem C. Exploring biofilm-forming bacteria for integration into BioCircuit wastewater treatment. *Eur Chem Biotechnol J* 2024;2:39–52. [\[CrossRef\]](#)
- [6] Liu H, Cheng S, Logan BE. Production of electricity from acetate or butyrate using a single-chamber microbial fuel cell. *Environ Sci Technol* 2005;39:658–662. [\[CrossRef\]](#)
- [7] Sonmez E, Avci B, Mohamed N, Bermek H. Investigation of performance losses in microbial fuel cells with low platinum loadings on air-cathodes. *Eur Chem Biotechnol J* 2024;1:11–26. [\[CrossRef\]](#)
- [8] Sukkasem C. Exploring biofilm-forming bacteria for integration into BioCircuit wastewater treatment. *Eur Chem Biotechnol J* 2024;2:39–52. [\[CrossRef\]](#)
- [9] Catal T, Yavaser S, Enisoglu-Atalay V, Bermek H, Ozilhan S. Monitoring of neomycin sulfate antibiotic in microbial fuel cells. *Bioresource Technol* 2018;268:116–120. [\[CrossRef\]](#)
- [10] Catal T, Kul A, Atalay VE, Bermek H, Ozilhan S, Tarhan N. Efficacy of microbial fuel cells for sensing of cocaine metabolites in urine-based wastewater. *J Power Sources* 2019;414:1–7. [\[CrossRef\]](#)
- [11] Fan Y, Janicek A, Liu H. Stable and high voltage and power output of CEA-MFCs internally connected in series (iCiS-MFC). *Eur Chem Biotechnol J* 2024;1:47–57. [\[CrossRef\]](#)
- [12] Berg KS, Palm P, Nielsen SD, Nygaard U, Bundgaard H, Rotvig C, Christensen AV. Acute symptoms in SARS-CoV-2 positive adolescents aged 15-18 years Results from a Danish national cross-sectional survey study. *Lancet Reg* 2022;100:354. [\[CrossRef\]](#)
- [13] Fumian TM, Malta FC, Dos Santos DRL, Pauvolid-Corrêa A, Fialho AM, Leite JPG, et al. SARS-CoV-2 RNA detection in stool samples from acute gastroenteritis cases, Brazil. *J Med Virol* 2021;93:2543–2547. [\[CrossRef\]](#)
- [14] Farman M, Akgul A, Sultan MRS, Asif H, Agarwal P, Hassani MK. Numerical study and dynamics analysis of diabetes mellitus with co-infection of COVID-19 virus by using fractal fractional operator. *Scientific Reports* 2024;14:16489. [\[CrossRef\]](#)
- [15] Jamil S, Naik PA, Farman M, Saleem MU, Ganie AH. Stability and complex dynamical analysis of COVID-19 epidemic model with non-singular kernel of Mittag-Leffler law. *J Appl Mat Comput* 2024;70:3441–3476. [\[CrossRef\]](#)
- [16] Izquierdo-Lara R, Elsinga G, Heijnen L, Munnink BBO, Schapendonk CME, Nieuwenhuijse D, et al. Monitoring SARS-CoV-2 Circulation and Diversity through Community Wastewater Sequencing, the Netherlands and Belgium. *Emerg Infect Dis* 2021;27:1405–1415. [\[CrossRef\]](#)
- [17] Zamhuri SA, Soon CF, Nordin AN, Rahim RA, Sultana N, Khan MA, et al. A review on the contamination of SARS-CoV-2 in water bodies: Transmission route, virus recovery and recent bio-sensor detection techniques. *Sens Bio-Sens Res* 2022;100:482. [\[CrossRef\]](#)

- [18] Reynolds LJ, Gonzalez G, Sala-Comorera L, Martin NA, Byrne A, Fennema S, et al. SARS-CoV-2 variant trends in Ireland: Wastewater-based epidemiology and clinical surveillance. *Sci Total Environ* 2022;155828. [\[CrossRef\]](#)
- [19] Zahmatkesh S, Amesho KT, Sillanpää M. A critical review on diverse technologies for advanced wastewater treatment during SARS-CoV-2 pandemic: What do we know? *J Hazardous Mater Adv* 2022;7:100121. [\[CrossRef\]](#)
- [20] Škulcová AB, Tamášová K, Staňová AV, Bírošová L, Krahulcová M, Gál M, et al. Effervescent ferrate(VI)-based tablets as an effective means for removal SARS-CoV-2 RNA, pharmaceuticals and resistant bacteria from wastewater. *J Water Proc Eng* 2021;43:102223. [\[CrossRef\]](#)
- [21] Ahmed W, Angel N, Edson J, Bibby K, Bivins A, O'Brien JW, et al. First confirmed detection of SARS-CoV-2 in untreated wastewater in Australia: A proof of concept for the wastewater surveillance of COVID-19 in the community. *Sci Total Environ* 2020;728:138764. [\[CrossRef\]](#)
- [22] Guerrero-Esteban T, Gutiérrez-Sánchez C, Villamanso AM, Revenga-Parra M, Pariente F, Lorenzo E. Sensitive SARS-CoV-2 detection in wastewaters using a carbon nanodot-amplified electrochemiluminescence immunosensor. *Talanta* 2022;247:123543. [\[CrossRef\]](#)
- [23] Miyani B, Fonoll X, Nortan F, Mehrotra A, Xagorarakis I. SARS-CoV-2 in Detroit Wastewater. *J Environ Manage* 2020;146:06020004. [\[CrossRef\]](#)
- [24] Wurtzer S, Marechal V, Mouchel JM, Maday Y, Teyssou R, Richard E, et al. Evaluation of lockdown effect on SARS-CoV-2 dynamics through viral genome quantification in waste water. *Euro Surveill* 2020;25:pil=2000776. [\[CrossRef\]](#)
- [25] D'Aoust PM, Mercier E, Montpetit D, Jia JJ, Alexandrov I, Neault N, et al. Quantitative analysis of SARS-CoV-2 RNA from wastewater solids in communities with low COVID-19 incidence and prevalence. *Water Res* 2021;188:116560. [\[CrossRef\]](#)
- [26] Al-Gheethi A, Al-Sahari M, Malek MA, Noman E, Al-Maqtari Q, Mohamed R, et al. Disinfection Methods and Survival of SARS-CoV-2 in the Environment and Contaminated Materials: A Bibliometric Analysis. *Sustainability* 2020;12:7378. [\[CrossRef\]](#)
- [27] Ahmed W, Bivins A, Smith WJM, Metcalfe S, Stephens M, Jennison AV, et al. Detection of the Omicron (B.1.1.529) variant of SARS-CoV-2 in aircraft wastewater. *Sci Total Environ* 2022;820:153171. [\[CrossRef\]](#)
- [28] Wilhelm A, Schoth J, Meinert-Berning C, Agrawal S, Bastian D, Orschler L, et al. Wastewater surveillance allows early detection of SARS-CoV-2 omicron in North Rhine-Westphalia, Germany. *Sci Total Environ* 2022;846:157375. [\[CrossRef\]](#)
- [29] Van Poelvoorde LAE, Gobbo A, Nauwelaerts SJD, Verhaegen B, Lesenfants M, Janssens R, et al. Development of a reverse transcriptase digital droplet polymerase chain reaction-based approach for SARS-CoV-2 variant surveillance in wastewater. *Water Environment research: a research publication of the Water Environment Federation* 2024;96:e10999. [\[CrossRef\]](#)
- [30] Kallem P, Hegab H, Alsafar H, Hasan SW, Banat F. SARS-CoV-2 detection and inactivation in water and wastewater: review on analytical methods, limitations and future research recommendations. *Emerg Microbes Infect* 2023;12:2222850. [\[CrossRef\]](#)
- [31] Pasternak G, Greenman J, Ieropoulos I. Removal of Hepatitis B virus surface HBsAg and core HBcAg antigens using microbial fuel cells producing electricity from human urine. *Sci Rep* 2019;9:11787. [\[CrossRef\]](#)
- [32] Cheng S, Liu H, Logan BE. Increased performance of single-chamber microbial fuel cells using an improved cathode structure. *Electrochem Commun* 2006;8:489–494. [\[CrossRef\]](#)
- [33] Catal T, Li K, Bermek H, Liu H. Electricity production from twelve monosaccharides using microbial fuel cells. *J Power Sources* 2008;175:196–200. [\[CrossRef\]](#)
- [34] Lovley DR, Phillips EP. Novel mode of microbial energy metabolism: organic carbon oxidation coupled to dissimilatory reduction of iron or manganese. *App Environ Microbiol* 1988;54:1472–1480. [\[CrossRef\]](#)
- [35] Catal T, Lesnik KL, Liu H. Suppression of methanogenesis for hydrogen production in single-chamber microbial electrolysis cells using various antibiotics. *Bioresour Technol* 2015;187:77–83. [\[CrossRef\]](#)
- [36] Bar-Or I, Indenbaum V, Weil M, Elul M, Levi N, Aguvaev I, et al. National Scale Real-Time Surveillance of SARS-CoV-2 Variants Dynamics by Wastewater Monitoring in Israel. *Viruses* 2022;14:1229. [\[CrossRef\]](#)
- [37] Sonmez E, Avci B, Mohamed N, Bermek H. Investigation of performance losses in microbial fuel cells with low platinum loadings on air-cathodes. *Eur Chem Biotechnol J* 2024;1:11–26. [\[CrossRef\]](#)
- [38] Acosta N, Bautista MA, Hollman J, McCalder J, Beudet AB, Man L, et al. A multicenter study investigating SARS-CoV-2 in tertiary-care hospital wastewater. viral burden correlates with increasing hospitalized cases as well as hospital-associated transmissions and outbreaks. *Water Research* 2021;201:117369. [\[CrossRef\]](#)
- [39] Tandukar S, Sthapit N, Thakali O, Malla B, Sherchan SP, Shakya BM, et al. Detection of SARS-CoV-2 RNA in wastewater, river water, and hospital wastewater of Nepal. *Sci Total Environ* 2022;824:153816. [\[CrossRef\]](#)

- 
- [40] Catal T, Kavanagh P, O’Flaherty V, Leech D. Generation of electricity in microbial fuel cells at sub-ambient temperatures. *J Power Sour* 2011;196:2676–2681. [\[CrossRef\]](#)
- [41] Emalya N, Tarmizi S, Munawar E, Fellner J, Yunardi. Coupling electrochemical energy generation with leachate bioremediation in sediment microbial fuel cell reactors. *Case Stud Chem Environ Eng* 2024;10:100896. [\[CrossRef\]](#)
- [42] Akagunduz D, Aydin O, Tuncay E, Bermek H. Microbial fuel cells: A potent and sustainable solution for heavy metal removal. *Eur Chem Biotechnol J* 2025;1:45–69. [\[CrossRef\]](#)
- [43] Catal T, Liu H. Microbial fuel cell technology: Novelties for a clean future. *Eur Chem Biotechnol J* 2025;1:1–20. [\[CrossRef\]](#)